Activation of Silane by W+ in the Gas Phase: Fourier-Transform Ion Cyclotron Resonance and ab Initio Theoretical Studies

ARTICLE *in* JOURNAL OF THE AMERICAN CHEMICAL SOCIETY · JUNE 1996

Impact Factor: 12.11 · DOI: 10.1021/ja952221o

3 AUTHORS:

Ferhati Azedine
The University of Batna
12 PUBLICATIONS **68** CITATIONS
SEE PROFILE

Terrance Mcmahon
University of Waterloo
206 PUBLICATIONS **5,438** CITATIONS
SEE PROFILE

Gilles Ohanessian
French National Centre for Scientific Research
115 PUBLICATIONS **3,705** CITATIONS
SEE PROFILE

Activation of Silane by W^+ in the Gas Phase: Fourier-Transform Ion Cyclotron Resonance and ab Initio Theoretical Studies

A. Ferhati, T. B. McMahon,[†] and G. Ohanessian*

Contribution from the Laboratoire des Mécanismes Réactionnels, URA 1307 du CNRS, Ecole Polytechnique, 91128 Palaiseau Cedex, France

Received July 6, 1995[⊗]

Abstract: The gas-phase reactions of the bare tungsten cation W^+ with silane have been investigated using Fourier-Transform Ion Cyclotron Resonance mass spectrometry. Dehydrogenation of a first molecule leads to the formation of $WSiH_2^+$. This ion is itself reactive with a second silane molecule, this time through elimination of $2H_2$, to form $WSi_2H_2^+$. A similar reaction follows, yielding $WSi_3H_2^+$ as the next product ion, which itself leads to both $WSi_4H_4^+$ and $WSi_4H_2^+$. This seems to initiate two parallel reaction sequences, yielding $WSi_{10}H_6^+$ as the major final product, together with a minor amount of $WSi_{10}H_4^+$. CID experiments on the products of the first three reactions were carried out to aid in their structural elucidation. Ab initio calculations at the CASSCF level have been performed in order to derive optimum structures for the first two product ions $WSiH_2^+$ and $WSi_2H_2^+$, and for the non-observed intermediate $WSi_2H_4^+$. The results show that structural isomerism exists for these three ions, due to the versatile bonding capabilities of W^+ and Si. The ground state of $WSiH_2^+$ is a high-spin (sextet) silylene complex in which there is a dative bond between SiH_2 and the metal. For $WSi_2H_4^+$ there are two low-energy isomers, a covalently bonded metal disilene three-membered ring with a quartet spin state, and a datively bonded metal silylsilylene in a high-spin sextet. It is proposed that the successive ions formed have compact structures, and that the reaction sequence ends when the metal gets trapped into a silicon cage, or alternatively when it no longer has enough nonbonding electrons to insert exothermically into a Si−H bond of a further silane molecule.

Introduction

Activation of small molecules by transition metals is much more common in the gas phase, where the generation of highly unsaturated metal centers is straightforward, than it is in the condensed phase. A large body of data has now been accumulated on reactions involving activation of C−C, C−H, X−H, ... bonds.[1] Loss of H_2, alkanes, and other saturated neutral fragments results in the formation of ionic complexes bearing unsaturated ligands.

An intriguing aspect of such activation which has emerged in recent years is the possibility that a chain of reactions may occur after the first activation step. Several such sequences have already been observed. Since the early report by Carlin et al.[2] that various first-row metal cations activate as many as eight ethylene sulfide molecules to generate metal polysulfide ions, secondary reactions have also been observed in, for example, the activation of alkanes by group 5 cations,[3] Zr^+,[4] and several doubly charged ions.[4,5] Nb^+ and Ta^+ have also been found recently to react with three and four benzene molecules, respectively.[6] Schröder et al. have described a sequence of four dehydrogenations of ethylene by Fe^+.[7] Halobenzenes undergo sequential reactions with several first-row metal cations.[8] We have observed such chains for all simple alkanes and alkenes reacting with W^+ [9a,b] and $W(CO)^+$ [9c] with nine steps at least in the cases of allene and propyne.[10] The longest sequence observed to date appears to be the Ti^+-induced oligomerization of ethene, which involves >20 neutral molecules in a flow tube experiment.[11] However, four molecules at most were activated (dehydrogenated), the other reactions being simple additions. Ta^+ also induces a dehydrogenation sequence with ethylene, leading to the formation of $TaC_{20}H_n^+$ ($n = 14, 16, 18$) after ten reactions.[12] The requirements for the occurrence of such reactions are as yet unclear, as are the reasons for the chain termination.

[†] On sabbatical leave from the Department of Chemistry, University of Waterloo, Waterloo, Ontario, Canada N2L3G1 (1991−92).

[⊗] Abstract published in *Advance ACS Abstracts,* May 1, 1996.

(1) Selected reviews include the following: (a) Eller, K.; Schwarz, H. *Chem. Rev.* **1991**, *91*, 1121. (b) Allison, J. *Prog. Inorg. Chem.* **1986**, *34*, 627. (c) Buckner, S. W.; Freiser, B. S. *Polyhedron* **1988**, *7*, 1583. (d) Armentrout, P. B.; Beauchamp, J. L. *Acc. Chem. Res.* **1989**, *22*, 319. (e) *Gas Phase Inorganic Chemistry*; Russell, D. H., Ed.; Plenum: New York, 1989. (f) Armentrout, P. B. *Annu. Rev. Phys. Chem.* **1990**, *41*, 313. (g) Weissshaar, J. C. In *Gas Phase Metal Reactions*; Fontijn, A., Ed.; North Holland: Amsterdam, 1992; p 253. (h) Bowers, M. T. *Acc. Chem. Res.* **1994**, *27*, 324.

(2) Carlin, T. J.; Wise, M. B.; Freiser, B. S. *Inorg. Chem.* **1981**, *20*, 2743.

(3) (a) Jackson, T. C.; Carlin, T. J.; Freiser, B. S. *J. Am. Chem. Soc.* **1986**, *108*, 1120. (b) Buckner, S. W.; McMahon, T. J.; Byrd, G. D.; Freiser, B. S. *Inorg. Chem.* **1989**, *28*, 3511.

(4) Ranasinghe, Y.; McMahon, T. J.; Freiser, B. S. *J. Phys. Chem.* **1991**, *95*, 7721.

(5) Gord, J. R.; Freiser, B. S.; Buckner, S. W. *J. Chem. Phys.* **1989**, *91*, 7530.

(6) Pope, R. M.; VanOrden, S. L.; Cooper, B. T.; Buckner, S. W. *Organometallics* **1992**, *11*, 2001.

(7) Schröder, D.; Sulzle, D.; Hrusak, J.; Böhme, D. K.; Schwarz, H. *Int. J. Mass Spectrom. Ion Proc.* **1991**, *110*, 145.

(8) (a) Dietz, T. G.; Chatellier, D. S.; Ridge, D. P. *J. Am. Chem. Soc.* **1978**, *100*, 4905. (b) Bjarnason, A.; Taylor, J. W. *Organometallics*, **1989**, *8*, 2020. (c) Bjarnason, A. *Organometallics*, **1991**, *10*, 1244. (d) Huang, Y.; Freiser, B. S. *J. Am. Chem. Soc.* **1989**, *111*, 2387. (e) Huang, Y.; Freiser, B. S. *J. Am. Chem. Soc.* **1990**, *112*, 1682.

(9) (a) Ferhati, A.; McMahon, T. B.; Ohanessian, G. *Trends Inorg. Chem.* **1993**, *3*, 151. (b) Mourgues, P.; Ferhati, A.; McMahon, T. B.; Ohanessian, G. In preparation. (c) Mourgues, P.; Ohanessian, G. *Rapid Commun. Mass Spectrom.* **1995**, *9*, 1201.

(10) Ferhati, A.; Sozzi, G.; Ohanessian, G. *Org. Mass. Spectrom.* **1993**, *28*, 1453.

(11) Guo, B. C.; Castleman, A. W. *J. Am. Chem. Soc.* **1992**, *114*, 6152.

(12) Cassady, C. J.; McElvany, S. W. *J. Am. Chem. Soc.* **1990**, *112*, 4788.

S0002-7863(95)02221-9 CCC: $12.00

In a systematic Fourier-Transform Ion Cyclotron Resonance (FT-ICR) study of the reactivity of third-row transition metal cations with methane,[13] Irikura and Beauchamp have shown that Ta^+, W^+, Os^+, Ir^+, and Pt^+ are all able to dehydrogenate sequentially several CH_4 molecules. This is probably due to the stronger bonds formed by third-row metal ions compared to their first- and second-row congeners.[14] The sequences observed involve a varying number of methane molecules, for which there is no explanation yet.

The energetic requirement for exothermic dehydrogenation of methane, reaction 1, is difficult to satisfy:[15]

$$CH_4\,(^1A_1) \rightarrow CH_2\,(^3B_2) + H_2 \qquad \Delta H = 111\ \text{kcal·mol}^{-1} \quad (1)$$

It is, however, much less stringent for silane dehydrogenation, reaction 2:

$$SiH_4\,(^1A_1) \rightarrow SiH_2\,(^1A_1) + H_2 \qquad \Delta H = 55\ \text{kcal·mol}^{-1} \quad (2)$$

It is therefore expected that sequential activation of several silane molecules would be more facile than that with methane, and alkanes in general, especially with third-row metal ions. As recalled below, there is a growing body of evidence that this is indeed the case.

In an ion beam apparatus, Ni^+, Co^+, and Ti^+ have been found to yield exothermically the single dehydrogenation product $MSiH_2^+$, while at low ion kinetic energies V^+, Cr^+, and Fe^+ are not reactive.[16] For comparison, none of the first-row metal cations is reactive with methane, and very few are able to dehydrogenate ethane exothermically.[1] More recently, the reactions of all first row and all group 2 metal cations with silane have been re-investigated in a guided ion beam spectrometer.[17] In all cases except Mn^+, dehydrogenation was found to be the prevalent reaction channel at low ion kinetic energies. Varying the ion source conditions allowed the determination of state-specific results, including bond energies, in many of these case. Primary reactions of metals with various organosilanes have also been reported.[16,18,19]

The single-collision conditions of the above experiments have left open the question of subsequent reactivity of $MSiH_2^+$ with other silane molecules. Sequential dehydrogenation of silane was observed for the first time with Y^+.[20] This ion reacts with at least seven silane molecules to yield $YSi_nH_{2n}^+$ and $YSi_nH_{2n-x}^+$ ions, with the precise end of reaction being difficult to determine. In contrast, reaction with Sc^+ was found to be endothermic, and the successive activation of three SiH_4 molecules to be slow.[21] In the same study, Lu^+ was found to be unreactive. Os^+ has also been reported to react sequentially with three SiH_4 molecules, yielding $OsSi_n^+$ ($n = 1-3$) as major products and $OsSi_nH_2^+$ as minor products.[22] With the range of reaction times considered, no Si_4 product was observed. We have recently reported[23] on the sequential reactions of W^+ with ten silane molecules. This appears to be the longest reaction sequence observed with silane in the gas phase to date. Reactions were shown to be fast and to involve extensive dehydrogenation of silane, leading to $WSi_{10}H_6^+$ and a smaller amount of $WSi_{10}H_4^+$ as final products. In this paper, we report full details of the FT-ICR study of this reaction sequence. The kinetics of reaction are studied in detail, and collision-induced dissociation (CID) spectra have been recorded whenever possible in order to help derive plausible structures for the various ions formed. It is, however, impossible to eliminate all possible structures but one for a given formula. We have therefore performed ab initio calculations on some of these ions, in order to gain more structural and energetic information.

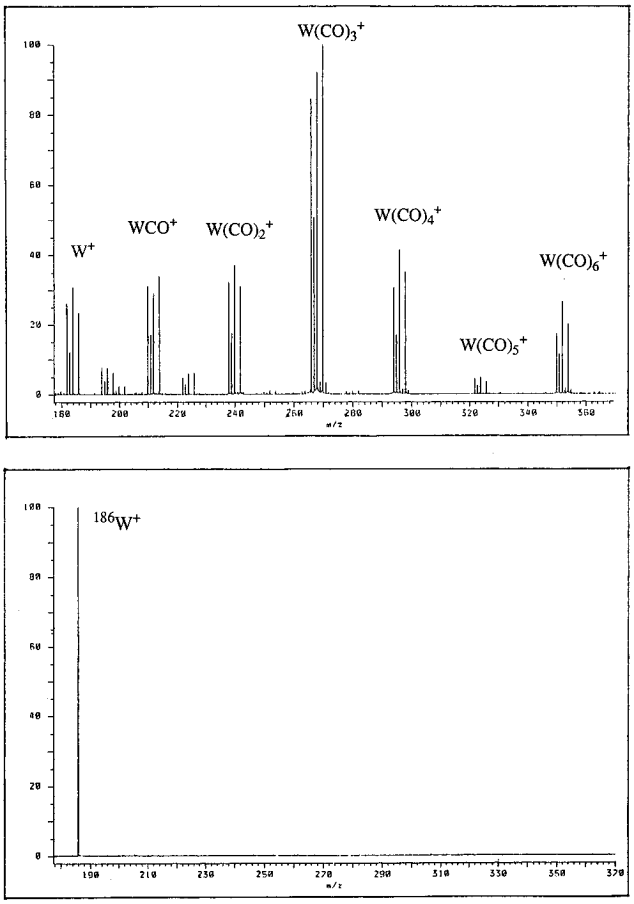

Figure 1. (a) Electron impact spectrum of $W(CO)_6$. (b) Selection of $^{186}W^+$ after ejection of $W(CO)_x^+$ ($x = 1-6$), WC_x^+ ($x = 1-3$), and other isotopes of W^+.

Experimental Section

All experiments were carried out on a Bruker Spectrospin CMS-47X FT-ICR mass spectrometer. Electron impact (EI) on $W(CO)_6$ (with electron energies in the 50−70 eV range) in an external ion source[24] generates $W(CO)_n^+$ ions ($n = 0-6$), see Figure 1a. Among these, the

(13) (a) Irikura, K. K.; Beauchamp, J. L. *J. Am. Chem. Soc.* **1991**, *113*, 2769. (b) Irikura, K. K.; Beauchamp, J. L. *J. Phys. Chem.* **1991**, *95*, 8344.

(14) (a) Ohanessian, G.; Brusich, M. J.; Goddard, W. A. *J. Am. Chem. Soc.* **1990**, *112*, 7179. (b) Ohanessian, G.; Goddard, W. A. *Acc. Chem. Res.* **1990**, *23*, 386.

(15) (a) Lias, S. G.; Bartmess, J. E.; Liebman, J. F.; Holmes, J. L.; Levin, R. D.; Mallard, W. G. *J. Phys. Chem. Ref. Data Suppl.* **1988**, *17*, No. 1. (b) Chase, M. W.; Davies, C. A.; Downey, J. R., Jr.; Frurip, D. J.; McDonald, R. A.; Syverud, A. N. *J. Phys. Chem. Ref. Data Suppl.* **1985**, *14*, No. 1. (c) See discussion in ref 17.

(16) Kang, H.; Jacobson, D. B.; Shin, S. K.; Beauchamp, J. L.; Bowers, M. T. *J. Am. Chem. Soc.* **1986**, *108*, 5668.

(17) (a) Kickel, B. L.; Armentrout, P. B. *J. Am. Chem. Soc.* **1994**, *116*, 10742. (b) Kickel, B. L.; Armentrout, P. B. *J. Am. Chem. Soc.* **1995**, *117*, 764. (c) Kickel, B. L.; Armentrout, P. B. *J. Am. Chem. Soc.* **1995**, *117*, 4057. (d) Kickel, B. L.; Armentrout, P. B. *J. Phys. Chem.* **1995**, *99*, 2024.

(18) (a) Karrass, S.; Schwarz, H. *Int. J. Mass Spectrom. Ion Proc.* **1990**, *98*, R1. (b) Karrass, S.; Schwarz, H. *Organometallics* **1990**, *9*, 2409. Hässelbarth, A.; Prüsse, T.; Schwarz, H. *Chem. Ber.* **1990**, *123*, 209, 213.

(19) (a) Jacobson, D. B.; Bakhtiar, R. *J. Am. Chem. Soc.* **1993**, *115*, 10830. (b) Bakhtiar, R.; Jacobson, D. B. *Organometallics* **1993**, *12*, 2876. (c) Bakhtiar, R.; Holznagel, C. M.; Jacobson, D. B. *J. Am. Chem. Soc.* **1993**, *115*, 345.

(20) Decouzon, M.; Gal, J.-F.; Géribaldi, S.; Rouillard, M.; Sturla, J.-M. *Rapid Commun. Mass Spectrom.* **1989**, *3*, 298.

(21) Azzaro, M.; Breton, S.; Decouzon, M.; Geribaldi, S. *Rapid Commun. Mass Spectrom.* **1992**, *6*, 306.

(22) Irikura, K. K.; Beauchamp, J. L. *J. Am. Chem. Soc.* **1989**, *111*, 75.

(23) Ferhati, A.; McMahon, T. B.; Ohanessian, G. *Bull. Soc. Chim. Fr.* **1993**, *130*, 3.

(24) Kofel, P.; Allemann, M.; Kellerhals, Hp.; Wanczek, K. P. *Int. J. Mass Spectrom. Ion Proc.* **1985**, *65*, 97.

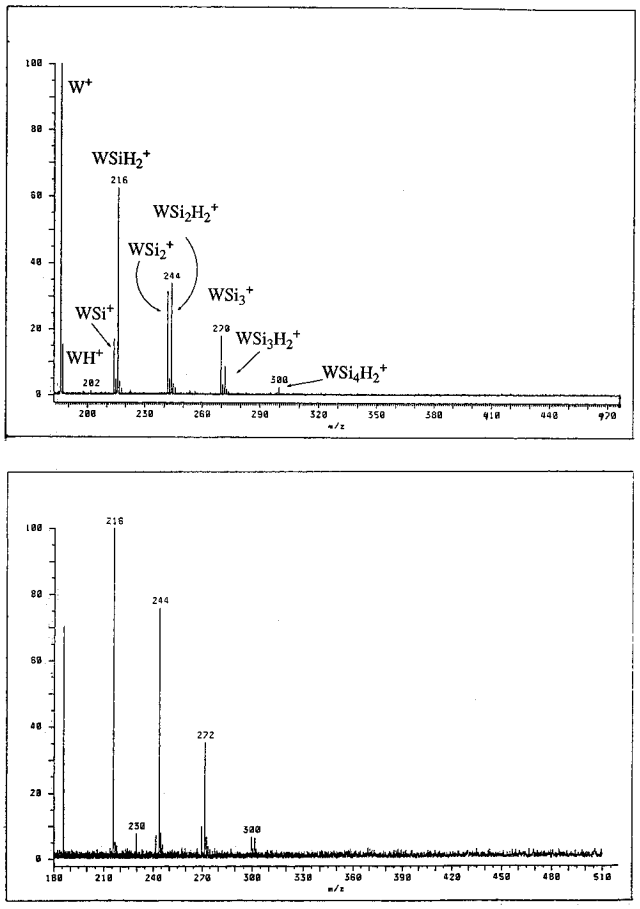

Figure 2. (a) Spectrum after 4 s of reaction, with a pressure of 5×10^{-8} mbar SiH_4 in the reaction cell. (b) Same as spectrum a in the presence of 10^{-6} mbar of argon in the cell.

desired W^+ amounts to ca. 10%. Using standard ejection techniques $^{186}W^+$ was isolated in the ICR cell (see Figure 1b) and allowed to react with SiH_4 present at 2.5×10^{-8} Torr.

Absolute pressures of SiH_4 and other gases used were obtained by the method outlined by Bartmess and Georgiadis.[25] Briefly, the ion gauge reading for methane was calibrated on the basis of the known bimolecular rate constants for reaction of CH_3^+ and CH_4^+ with methane. This gives a gauge correction factor for CH_4. The gauge correction factor for SiH_4 is thus proportional to the ratio of polarizabilities of SiH_4 and CH_4 times the CH_4 gauge correction factor. This method is expected to yield SiH_4 pressures accurate to within 10%. A value of 4.339 Å^3 [26] was used for the polarizability of silane. This value was also used to calculate the collision rate constants for ions with silane using the Langevin expression.[1f]

Thermalization of $^{186}W^+$ was ensured by collisions with argon present at a pressure of 10^{-6} Torr in the cell. The effect of collisional cooling is illustrated in Figure 2. Figure 2a shows the mass spectrum obtained without Ar at a reaction time of 4 s. Figure 2b shows the spectrum in the presence of Ar at the same reaction time. It can be seen that without thermalization a number of endothermic reaction channels are opened, leading to formation of WH^+ and WSi_n^+ ($n = 1-3$). In the presence of Ar, however, the only significant products observed are $WSi_nH_2^+$ ($n = 1-3$). Thus Ar acts as an efficient quencher of translational excitation of $^{186}W^+$. It is also noteworthy that when the ion kinetic energy is completely relaxed the reaction becomes faster as shown by the greater extent of reaction visible in Figure 2b vs Figure 2a. This phenomenon of a decreasing rate constant with increasing energy is very common for reactions involving complex potential energy surfaces with significant intermediate barriers.[27]

Concern has been expressed in the literature that ions generated by electron impact might contain a significant population of excited states.[28] In particular, recent studies of the reactions of Cr^+, the first-row congener of W^+, indicated important amounts of several excited states when obtained by EI from $Cr(CO)_6$ at 30−50 eV electron energies.[29] Some of the excited states, especially the ^{4}D and ^{4}G, exhibit reactivity with alkanes that differ vastly from that of the ^{6}S ground state. As was previously done by Ridge and co-workers,[30] we have monitored charge exchange between Cr^+ (generated by EI from $Cr(CO)_6$) and $Cr(CO)_6$. Whenever a mixture of states is present, the decay of the signal due to Cr^+ is a superposition of two or more exponential functions, corresponding to the reactions of the various states. Our experiments revealed that the lifetime of excited state (or states) of $^{52}Cr^+$ present is considerably longer than the 2-s minimum identified by Ridge et al. Under conditions where Cr^+ was first collisionally relaxed in Ar at 10^{-6} Torr for 10 s and then allowed to react further with $Cr(CO)_6$ for times up to 30 s, the presence of excited states was clearly evident from the non-single exponential decay observed.

In the case of W^+, spin−orbit coupling should lead to faster radiative relaxation of excited electronic states than for Cr^+. Thus collisions with Ar coupled with a significant time delay (see below) are more likely to thermalize W^+ efficiently to the ground state. The observed kinetics for reaction of W^+ with methane[9b] is very similar to that reported by Irikura and Beauchamp,[13] even though the latter experiments involved W^+ generated by laser ablation from a metal target. The observed decay of W^+ has the form of a single exponential, indicative of a reaction from a single reactive electronic state. A strong point against the presence of two reacting states arises from the deuterium isotope effect observed in the reaction of W^+ with methane. Reaction with CD_4 is observed to proceed 20 times more slowly than with CH_4, still with a single exponential decay of W^+. It is very unlikely that two states would react exactly at the same rate and with the same isotope effect. Thus we can safely conclude that our thermalization procedure generates negligible amounts of excited states.

There is another important difference between Cr^+ and W^+. In first-row transition metal ions, the very large difference in size of the 4s and 3d valence orbitals leads to very different reactivities for the states derived from the s^1d^{n-1} and d^n configurations. This has been illustrated for group 6 metals by the comparison of Cr^+ and Mo^+.[31] The latter is much more reactive, even though its ground state is ^{6}S (d^5) as for Cr^+, and the first excited state is ^{6}D (s^1d^4) for both with very similar splittings, 1.5 and 1.4 eV for Cr^+ and Mo^+, respectively.[32] In W^+, the ground state is ^{6}D rather than ^{6}S. It has been shown in the case of MH^+ hydrides[14] that third-row metal ions are able to extensively mix their valence 6s and 5d orbitals for bonding, because of their comparable sizes (due to the lanthanide contraction) and because the splitting between the lowest lying s^1d^{n-1}- and d^n-derived states is generally small (0.4 eV in W^+ when averaging over J states[32]). For W^+, we thus expect both ^{6}D and ^{6}S to lead to the same type of optimum binding, and therefore to have similar reactivities. If this is the case, then the presence of a minor population of the ^{6}S state would not be a problem.

A typical sequence is as follows: Ions produced by electron impact are transferred to the ICR cell, and are subjected first to a sequence of rf pulses to eliminate most undesired ions. After a short delay, a series of single frequency rf pulses are applied to eliminate the few remaining ions, especially those with *m*/*z* close to 186. A relaxation delay follows, after which a series of single frequency rf pulses are applied again to

(25) Bartmess, J. E.; Georgiadis, R. M. *Vacuum* **1983**, *33*, 149.
(26) See reference 19 in: Mandich, M. L.; Reents, W. D.; Jarrold, M. F. *J. Chem. Phys.* **1988**, *88*, 1703.
(27) Wolfgang, R. *Acc. Chem. Res.* **1969**, *2*, 248; **1970**, *3*, 48.
(28) (a) Halle, L. F.; Armentrout, P. B.; Beauchamp, J. L. *J. Am. Chem. Soc.* **1981**, *103*, 962. (b) Elkind, J. L.; Armentrout, P. B. *J. Chem. Phys.* **1986**, *84*, 4862. (c) Elkind, J. L.; Armentrout, P. B. *J. Chem. Phys.* **1987**, *86*, 1868. (d) Georgiadis, R.; Armentrout, P. B. *J. Phys. Chem.* **1988**, *92*, 7067. (e) Strobel, F.; Ridge, D. P. *J. Phys. Chem.* **1989**, *93*, 3635. (f) Armentrout, P. B. *Annu. Rev. Phys. Chem.* **1990**, *41*, 313. (g) Kemper, P. R.; Bowers, M. T. *J. Phys. Chem.* **1991**, *95*, 5134. (h) Oriedo, J. V. B.; Russell, D. H. *J. Phys. Chem.* **1992**, *96*, 5314. (i) Oriedo, J. V. B.; Russell, D. H. *J. Am. Chem. Soc.* **1993**, *115*, 8376.
(29) Fisher, E. R.; Armentrout, P. B. *J. Am. Chem. Soc.* **1992**, *114*, 2039, 2049.
(30) (a) Reents, W. D.; Strobel, F.; Freas, R. B.; Wronka, J.; Ridge, D. P. *J. Phys. Chem.* **1985**, *89*, 5666.
(31) Schilling, J. B.; Beauchamp, J. L. *Organometallics* **1988**, *7*, 194.
(32) Moore, C. B. *Tables of Atomic Energy Levels*; National Bureau of Standards: Washington, DC, 1971; Vols. II and III.

Table 1. Optimized Outer Core and Valence Basis Set for W^+

type	exponent	coeff
s	9.773	−0.075419
	7.475	0.266054
	3.4893	−0.862675
	1.2908	0.801433
	0.5759	1.0
	0.1382	1.0
	0.06539	1.0
p	25.59	−0.001881
	2.5054	−1.514192
	2.2153	1.601938
	0.7980	1.0
	0.3528	1.0
	0.1302	1.0
d	8.4483	−0.010333
	1.1683	0.228578
	0.8560	0.181351
	0.38659	1.0
	0.14105	1.0

eliminate any product ions formed during the thermalization delay. The reaction is then monitored as a function of time.

In order to help assign structures to some of the ions formed, collision induced dissociation (CID) spectra were recorded. A number of collision energies and observation delays were employed in each case (in the 10−50 eV energy range). Since isolation of a specific mass generally leads to translational excitation of ions with nearby masses, completely unambiguous CID experiments could be run for $WSi_nH_2^+$ ($n = 1-3$) only.

Computational Section

Ab initio calculations were run on some of the observed ions. All calculations used a Relativistic Effective Core Potential (RECP) for tungsten.[33] The use of a RECP not only reduces the number of basis functions in the calculations but also, and more importantly, enables the introduction of the main relativistic effects for the core electrons. The influence of these effects on the description of the valence electrons is known to be crucial.[34] We have optimized a flexible outer core and valence basis for W^+,[35] of the type (7s6p5d/4s4p3d). Since both the ground ^{6}D and first excited ^{6}S states involve singly occupied valence AO's, all exponents and contraction coefficients were optimized for the ground state energy, and are expected to be well suited for the ^{6}S state as well.[36] The valence p functions, corresponding to the description of an orbital that is empty in the ground state, were optimized for the lowest p^1d^4 state and then scaled by 1.2 to obtain valence functions.[37] These p functions are expected to play the role of polarization functions for s orbitals at the SCF level, and to help describe the angular correlation of s and d electrons at the CI level. The resulting basis is given in Table 1. An additional f polarization function was determined in the form of a single Gaussian, in order to obtain more accurate energetics at the CI level. Optimization of its exponent for the total CASSCF energy of $WSiH_2^+$ at the optimum structure of **1** $^4B_1$ led to a value of 0.225.

Calculations on $WSiH_2^+$ used the all-electron 6-31G* basis on Si[38] with a d exponent of 0.42. For larger ions, the ECP of Stevens et al. was used, with the associated split-valence plus polarization basis.[39] The use of an ECP on Si not only reduces the size of computations but also leads to much easier convergence in MCSCF calculations on ions involving two or more silicon atoms. The reliability of calculations using an ECP was tested by comparing the silylene structure obtained for $WSiH_2^+$ (**1** $^4B_1$) with that obtained using the all-electron 6-31G* basis. The W−Si length is 2.403 and 2.404 Å, the Si−H length is 1.505 and 1.509 Å, and the WSiH bond angle is 123.03 and 123.05°, at the 6-31G* and ECP levels, respectively. Thus the use of an ECP leads to very limited structural deviations, which correspond to negligible energy differences: the ECP energies at the 6-31G* and ECP geometries differ by 10^{-5} hartrees.

The hydrogen basis is the standard unscaled Huzinaga−Dunning (4s/2s) set,[40] except for $WSiH_2^+$ in which case a p function with exponent 0.5 was added to the DZ basis. This was done because the hydrogens are bound to tungsten in some of the structures, which might require extra flexibility for the description of the W−H bond(s).

Unrestricted Hartree−Fock (UHF) and Restricted Open-shell Hartree−Fock (ROHF) were initially performed on some of the ions. It was systematically observed that a very large spin contamination occurs in UHF calculations. While this problem is avoided a priori with ROHF calculations, the wave function is likely not able to describe bonding accurately either. For this reason, most of the results reported in this paper were obtained through Complete Active Space Self-Consistent Field (CASSCF) calculations. In some cases (structures of low symmetry), the CASSCF method led to configuration lists that were too large to be tractable, especially for low-spin states such as doublets. For instance for the quartet and doublet states of $WSiH_2^+$, the active space comprised all 11 valence electrons in 11 orbitals, and the full CASSCF involves 20000−27000 Configuration State Functions (CSF) in C_{2v} symmetry, depending on spatial symmetry and spin multiplicity. Such wave functions would be intractable in C_s symmetry, and therefore the level of excitation was restricted to four at the most (SDTQ CI) for C_s structures. Such wave functions have the drawback of more difficult energy convergence as compared to CASSCF. In larger ions, all structures considered have the hydrogens bonded to silicon atoms, and correlating the Si−H bonds was not considered important. Thus the active space included the W−Si and Si−Si bonds, plus the nonbonding electrons on tungsten.

All structures were obtained by full gradient optimization at the CASSCF level, within symmetry constraints as indicated in each case. In most cases, the wave functions are much too complex to be amenable to a vibrational analysis which would assess whether optimized structures are true minima on the potential energy surfaces. A careful exploration of many portions of the surfaces was carried out in order to ensure that the lowest minima were located. Exceptions to this are the sextet states of isomers of $WSiH_2^+$ and $WSi_2H_2^+$ and all states of $WSi_2H_4^+$. Because of the complexity of the CASSCF wave functions, calculations of the full reaction pathways turned out to be impossible, expecially since transition states are most often structures with no spatial symmetry.

Computations were carried out using the HONDO 8.1 package[41] on an IBM 9121-260 mainframe computer and on a IBM RISC/6000 560 workstation.

Results

The entire sequence of reactions can be appropriately divided into two parts. The first involves the activation of the first three silane molecules, while the second includes the fourth to tenth (last) reaction steps.

The First Three Reactions. Each of the first three reactions yields a single product as described in reactions 3−5:

(33) Ross, R. B.; Powers, J. M.; Atashroo, T.; Ermler, W. C.; LaJohn, L. A.; Christiansen, P. A. *J. Chem. Phys.* **1990**, *93*, 6654.

(34) Adequate references may be found in the compilation by Pyykkö, P. *Lecture Notes in Chemistry*; Springer-Verlag: Berlin, 1993; Vol. 60.

(35) (a) Restricted Hartree−Fock calculations in full atomic symmetry were run with the PSATOM package due to the Toulouse group. The version used was extensively modified by Prof. M. Pélissier. (b) Analogous basis sets have been previously optimized for Co^+, Rh^+, and Ir^+ and shown to yield accurate atomic spectra. See: Perry, J. K.; Goddard, W. A.; Ohanessian, G. *J. Chem. Phys.* **1992**, *97*, 7560.

(36) Rappé, A. K.; Smedley, T. A.; Goddard, W. A. *J. Phys. Chem.* **1981**, *85*, 2607.

(37) Wachters, A. J. H. *J. Chem. Phys.* **1970**, *52*, 1033.

(38) Gordon, M. S. *Chem. Phys. Lett.* **1980**, *76*, 163.

(39) Stevens, W. J.; Basch, H.; Krauss, M. *J. Chem. Phys.* **1984**, *81*, 6026.

(40) Dunning, T. H.; Hay, P. J. In *Methods of Electronic Structure Theory*; Schaefer, H. F., Ed.; Plenum: New York, 1977; Vol. 4, Chapter 1.

(41) HONDO-8 from MOTECC-90. Dupuis, M. et al. IBM Corp.: Yorktown Heights, NY, 1990.

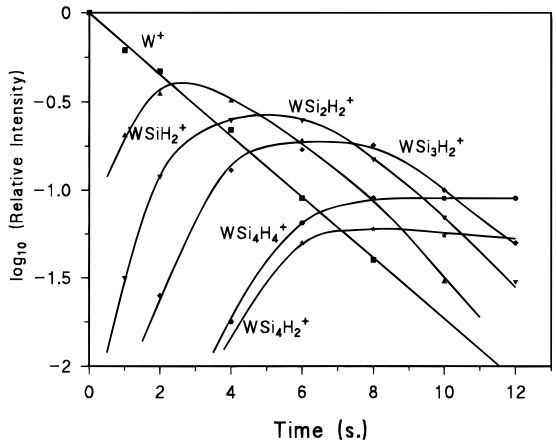

Figure 3. Relative intensities of observed peaks as a function of reaction time. Oxygen-containing species are not shown.

$$W^+ + SiH_4 \rightarrow WSiH_2^+ + H_2 \quad (3)$$

$$WSiH_2^+ + SiH_4 \rightarrow WSi_2H_2^+ + 2H_2 \quad (4)$$

$$WSi_2H_2^+ + SiH_4 \rightarrow WSi_3H_2^+ + 2H_2 \quad (5)$$

Kinetics of reactions are shown in Figure 3, with the appearance of the products of the fourth reaction also shown. The decay of the signal due to $^{186}W^+$ is exponential, indicative of the presence of a single reactive state (or, less probably of two reactive states with non-discernable reactivities with SiH_4). Each of the products forms and decays as the next reaction proceeds. As discussed below, all three reactions are fast and exothermic.

(a) $WSiH_2^+$ (m/z = 216). The rate constant for reaction 3 is determined to be 5.4×10^{-10} cm^3·molecule^{-1} s^{-1}, corresponding to ca. 50% of all collisions being reactive. There are several possible structures for $WSiH_2^+$, **1**−**6**.

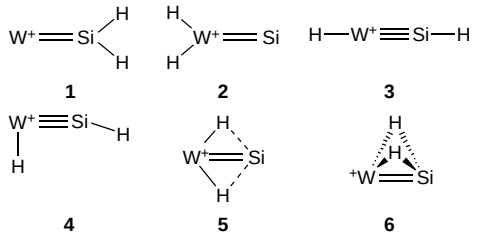

The CID spectrum of $WSiH_2^+$ shows loss of H_2 and of SiH_2, with the former being dominant. This is in contrast to the CID results of Kang et al.[16] for $CoSiH_2^+$, where loss of SiH_2 was largely dominant. This was used to propose the silylene structure as the most likely for $CoSiH_2^+$. It should be noted that the larger amount of H_2 loss is consistent with the much greater ability of W^+ to dehydrogenate many small molecules as compared to Co^+.[9,10] Thus any excess internal energy in the ion would be expected to lead to H_2 loss more easily for $WSiH_2^+$ than for $CoSiH_2^+$. Assuming a silylene structure for $WSiH_2^+$, the endothermicity of H_2 loss can be assumed to be approximately equal to that in $H_2C{=}SiH_2$, leading to H_2CSi plus H_2. This value has been calculated to be about 34 kcal/mol.[42] If the barrier in excess of this value is not very large, observation of H_2 loss in the CID spectrum of $WSiH_2^+$ is to be expected.

The possibility might also be considered that there is more than one structure present for $WSiH_2^+$. In order to explore this possibility, CID spectra were examined at a series of collision energies and collision times. The spectra showed that as the collision time or collision energy increases, the extent of fragmentation also increases but the ratio of W^+ and WSi^+ fragments remains constant. Thus the presence of two isomeric structures seems rather unlikely. The present results could be accommodated with several structures among **1**−**6** (except maybe **3** and **4** for which loss of H and/or SiH would be expected).

Ab initio calculations were performed on **1**−**6**. Since W^+ bears five valence electrons, all structures have nonbonding electrons at the metal (either five, three, or one, depending on whether W^+ makes zero, two, or four covalent bonds, respectively). This leads to a manifold of low-lying electronic states in each case. The nature of the ground state cannot generally be determined a priori. Thus calculations on the various possible states were performed for each structure, including geometry optimization for each state.

The electronic structure of **1** can be described as involving a W−Si double bond, of either σ/π or donation/back-donation type.[43] There remain three unpaired electrons on W^+, which can be arranged to form a quartet state in order to gain the largest exchange stabilization possible. With the molecule lying in the xz plane and the W−Si bond along the z axis, the W−Si σ bond is of a_1 symmetry and involves a s/d_σ hybrid at W^+, while the W−Si π bond is b_1 and involves the d_{yz} orbital at W^+. There are four valence orbitals left on tungsten in which the three unpaired electrons can be placed: d_{xz} (b_2), d_{xy} (a_2), and two combinations of s, d_{xx}, d_{yy}, and d_{zz} (a_1).[44] A manifold of quartet states is generated by singly occupying three orbitals out of these four, resulting in states of $^4A_2$, $^4B_1$, and $^4B_2$ symmetry. The geometry of the lowest state of each symmetry was optimized at the CASSCF level, and the results are summarized in Figure 4 and Table 2. The active space included all eleven valence electrons in eleven molecular orbitals: the four bonding pairs (with one bonding and one antibonding orbital for the description of each pair) plus the three singly occupied (high-spin coupled) orbitals on W^+. The Si−H bond lengths are close to 1.50 Å, slightly longer than typical because the non-dynamical correlation of these bond pairs is taken into account. In larger ions this is not so, and the lengths are close to the standard value of 1.48 Å.

The three states are close in energy, with $^4B_1$ being the lowest. In this state, the singly occupied metal orbitals are d_{xy}, d_{xz}, and a d_σ in the xz plane. $^4B_2$ is deduced from $^4B_1$ by replacing the d_{xy} singly occupied orbital by the $d_{x^2-y^2}$. Thus the electronic structures of the two states are very similar. In $^4A_2$, the larger s character in the high-spin orbitals leads to a longer bond in order to minimize electron repulsion (see Figure 4). This is probably why it is the highest state of the three. In all three states, the π bond is polarized toward W^+ (with roughly 1.35 electron on W and 0.65 on Si in the $^4B_1$ and $^4B_2$ states, and 1.25 and 0.75, respectively, in $^4A_2$). The total charge on W is ca. 0.7 in the three states. This is probably a sign that bonding is better described as σ and π covalent, rather than double charge transfer between ground state singlet SiH_2 (bearing a σ lone

(42) Allendorf, M. D.; Melius, C. F. *J. Phys. Chem.* **1992**, *96*, 428.

(43) (a) Cundari, T. R.; Gordon, M. S. *J. Phys. Chem.* **1992**, *96*, 631. (b) Nakatsuji, H.; Hada, M.; Kondo, K. *Chem. Phys. Lett.* **1992**, *196*, 404. (c) Musaev, D. G.; Morokuma, K.; Koga, N. *J. Chem. Phys.* **1993**, *99*, 7859. (d) Marquez, A.; Fernandez Sanz, J. *J. Am. Chem. Soc.* **1992**, *114*, 2903, 10019.

(44) All calculations used six d Cartesian components. Thus the a_1 orbitals are mixtures of s, d_{xx}, d_{yy}, and d_{zz}. In the text, the actual linear combinations are described as "in the xz plane" for a $d_{x^2-z^2}$ type orbital, "mainly in the y direction" for a d_{y^2}, i.e. $2d_{yy}-d_{xx}-d_{zz}$ type orbital, etc. Since all three d components have variationally determined coefficients, this is only a qualitative description of the wave function.

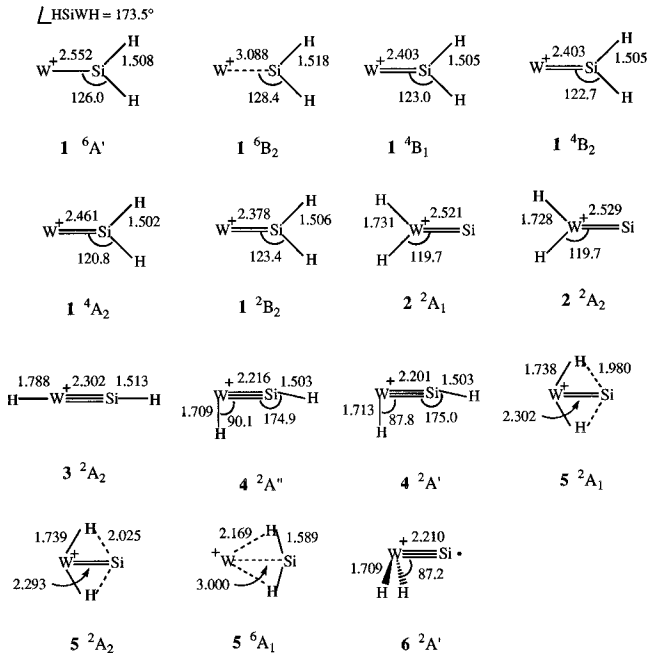

Figure 4. Optimized geometries for various electronic states of $WSiH_2^+$ isomers.

Table 2. Energies of Various Electronic States of $WSiH_2^+$ Isomers, Optimized at the CASSCF Level (See Text)

isomer and state	CSF[a]	total energy[b]	rel energy[c]
1 $^6A'$	12 160	−356.934 752	0.0
1 $^6B_2$	6 020	−356.889 932	26.1
1 $^4B_1$	20 531	−356.915 442	12.1
1 $^4B_2$	20 541	−356.912 702	13.8
1 $^4A_2$	20 627	−356.906 423	17.8
1 $^2B_2$	26 168	−356.869 961	40.6
2 $^2A_1$	26 640	−356.865 604	43.4
2 $^2A_2$	26 024	−356.863 838	44.5
3 $^2A_2$ ($^2\Delta$)	26 032	−356.854 703	50.2
4 $^2A'$	18 318	−356.915 965	11.8
4 $^2A''$	17 900	−356.906 904	17.5
5 $^2A_1$	26 640	−356.911 942	14.3
5 $^2A_2$	26 024	−356.908 049	16.7
5 $^6A_1$	6 086	−356.900 033	21.8
6 $^2A'$	17 988	−356.898 139	23.0

[a] Number of Configuration State Functions included in each case. [b] Total energies in atomic units (hartrees). [c] Relative energies in kcal/mol.

pair donating to W^+) and excited W^+ (bearing a π lone pair donating to SiH_2).[43]

Test calculations were also run on doublet states of **1**. It appears that the lowest-lying doublet states involve low-spin coupling of singly occupied orbitals analogous to those in quartet states, rather than doubly occupying one of the valence orbitals. A $^2B_2$ state with d_{xy}, d_{xz}, and s + d_σ singly occupied was optimized and found to lie 28.5 kcal/mol higher in energy than the ground $^4B_1$ state. Thus it appears that the exchange stabilization enjoyed by the quartets makes them significantly more stable than any doublet.

The W−Si bond length in **1** can be compared to the Ir−Si length in $IrSiH_2^+$, which was previously computed by Musaev et al.[43b] These authors, using a level of theory comparable to ours, obtained a bond length of 2.275 Å. Using the Christiansen core potential[33] and our own optimized basis for Ir^+ [35b] leads to a very similar value of 2.253 Å. The shorter Ir−Si bond compared to W−Si arises from the valence orbitals of Ir being smaller than those of W, due to its larger atomic number.

There is yet another alternative for binding a silylene group to W^+. The ground state of SiH_2 is $^1A_1$, with a σ lone pair, which explains why silicon is not as prone as carbon to making double bonds (since it requires, at least to a first approximation, an excitation of SiH_2 from $^1A_1$ to $^3B_1$[45]). Maintaining SiH_2 in its ground state requires an empty σ valence orbital on the metal for a strong dative interaction to be established. This is easily realized with W^+ which has five valence electrons in six valence orbitals. The other favorable aspect of such bonding is that W^+ can retain its high-spin, sextet character, with a large exchange stabilization. The drawback is that there is only one electron left in a π-type orbital, leading to a weak bond. Overall, there is a trade-off between weaker bonding and ground state fragments, compared to the quartet states. The ground sextet state of $WSiH_2^+$ resulting from the above building principles is a $^6A_1$ state. Full optimization at the CASSCF level shows that this is the ground state for the silylene structure, with an energy lower than that of $^4B_1$ by ca. 10 kcal/mol.[46] The vibrational analysis shows that bending the SiH_2 group out of the molecular plane would be stabilizing;[47] optimization of such a C_s structure leads to a further energy lowering of ca. 2 kcal/mol relative to the planar extremum, with a small bending angle and a slightly shorter W−Si bond length. It should be noted that further CI calculations yield a planar minimum, with a very small out-of-plane bending frequency. The CASSCF optimized structure of the $^6A'$ state is shown in Figure 4. The W−Si bond is significantly longer (by 0.15 Å) than in the $^4B_1$ state. It is thus clear that maintaining both W^+ and SiH_2 in their ground states has a decisive effect in lowering the energy of the $^6A'$.

Some additional information regarding the extent of charge tranfer in the $^6A'$ may be gained by investigating another sextet state, in which dative bonding is prevented. This is achieved by singly occupying all σ orbitals on the metal. The lowest such state is obtained when the only empty metal orbital is d_{xz} (in order to minimize repulsion with the Si−H bonds). The optimum geometry of this $^6B_2$ state (see Figure 4) has a much longer W−Si bond of 3.088 Å. The Mulliken charge on W is +0.72, while it is +0.53 in the $^6A'$ state, indicative of a significant charge transfer in the latter. The $^6B_2$ is higher than the $^6A'$ by 26.1 kcal/mol (Table 2). However this difference cannot be attributed solely to the difference in charge transfer. Since there is more repulsion in the σ space, the W−Si length is stretched and the electrostatic interaction between W^+ and SiH_2 is also weakened.

The electronic structure of **2** involves two W−H covalent bonds, described by two combinations of W−H bonding orbitals, one of a_1 symmetry (s/d_σ hybrid at W^+) and one which is b_2 (d_{xz} at W^+). Since the d_{xz} orbital is already "in use", it cannot form an in-plane π interaction with the p_x orbital on Si, so that the W−Si bond is a double, not a triple, bond. This leaves a lone pair on the silicon, in an orbital with mainly s character, while the p_x orbital is empty. There remain two tungsten orbitals in which one unpaired electron must be placed, d_{xy} (a_2) and $d_{x^2-y^2}$ (a_1), leading to low-lying $^2A_2$ and $^2A_1$ states, respectively. The active space again comprised all eleven valence electrons in eleven orbitals, with bonding/antibonding combinations for the description of the four bond pairs. The Si lone pair uses the empty p_x as correlating orbital.

The $^2A_1$ and $^2A_2$ states are very similar at the CASSCF level (see Figure 4), with $^2A_1$ lower in energy by only 1.6 kcal/mol. The geometries are very similar for both states, with W−H

(45) Horowitz, D. S.; Goddard, W. A. *J. Mol. Struct. (Theochem)* **1988**, *163*, 207.

(46) A detailed discussion of these two bonding modes has been given in the case of metal−methylene complexes: Carter, E. A.; Goddard, W. A. *J. Am. Chem. Soc.* **1986**, *108*, 2180, 4746.

(47) Trinquier, G.; Malrieu, J. P. In *The Chemistry of Double-bonded Functional Groups*; Patai, S., Ed.; John Wiley and Sons: New York, 1989; Supplement A, Vol. 2, Chapter 1.

bonds of ca. 1.73 Å (close to the value in WH^+, 1.701 Å[14]), trigonal structure at tungsten, and a W−Si double bond somewhat longer than in **1**. Their energies are significantly higher than for all states of **1**; this can be related to the W−H bonds being weaker than the Si−H bonds, and to a loss of exchange stabilization on W^+ in doublet states relative to quartets.

However **2** is likely not to be the absolute minimum on both the $^2A_2$ and $^2A_1$ potential surfaces. Instead we find that the di-bridged form **5** is of significantly lower energy. Here the H atoms point toward the Si, and there is a stabilizing interaction between the out-of-phase combination of W−H bonding orbitals and the empty p_x orbital on Si. While the W−H bond lengths are nearly the same as in **2**, the W−Si bond is shortened by more than 0.2 Å in order to enhance stabilization. This leads to nonbonded Si−H distances of about 2 Å. This type of distortion, while not very common, is not new. It has been discussed for example in Si_2H_2 and $Si_2H_2^+$.[48] Strong distortion from classical hybridization is common in unsaturated silicon compounds. It is also easy at unsaturated transition metal centers which have a manifold of valence orbitals available for bonding in different directions.

High-spin states were also considered for **2** and **5**. The interaction takes place between WH_2^+ in its ground quartet state and Si in its ground triplet state, leading to an overall sextet. In **2**, this leads to energies higher than those for the doublet states, so the results are not detailed here. In **5**, all attempts on quartet states lead to higher energy species. On the sextet surface, geometry optimization slowly leads to a structure in which both hydrogens are bound to Si rather than to W^+. The lowest, $^6A_1$, state corresponds to the interaction of SiH_2 (singlet) with W^+ in its ground sextet, with an empty s/d_σ orbital. The Si−H bonds are stretched compared to those in free SiH_2 (see Figure 4), corresponding to an agostic interaction with W^+. This sextet state is slightly higher in energy than the doublets, and lies 21.8 kcal/mol higher than the ground sextet of the metal−silylene structure. The potential surface is very flat in this area, and distortions leading to C_s structures with one short Si−H bond and one short W−H bond are slightly stabilizing. It is likely that this sextet is a local minimum and is connected to the sextet silylene structure by an energy barrier corresponding to inversion at Si.

Structures **3** and **4**, with one hydrogen bonded to each heavy atom, were also considered. In such cases there is a triple bond between tungsten and silicon; it involves a s/d_σ hybrid and the d_{xz} and d_{yz} tungsten orbitals. There remain the d_{xy} and $d_{x^2-y^2}$ orbitals on W^+ in which to place one nonbonding electron. In the linear structure **3**, these two possibilities lead to degenerate components of a $^2\Delta$ state. In **4**, symmetry is reduced to C_s, and two distinct states of $^2A''$ and $^2A'$ symmetry emerge.

In **3**, W^+ makes two covalent bonds to Si and H with its s and d_{zz} orbitals. Since the two bonding orbitals have to be orthogonal, hybridization cannot be optimal. In **4** the d_σ along the *x* axis is properly oriented to mix in the W−H bonding orbital while the d_σ along the *z* axis participates in the W−Si bond. This allows more flexible hybridization at tungsten. As a result, both the W−Si and the W−H bonds are significantly strengthened, as illustrated by the decrease of their lengths (ca. 0.08 Å for each). The reinforced bonding interactions lead to a large stabilization for both the $^2A'$ and $^2A''$ states, of 32.8 kcal/mol, making structure **4** in its $^2A'$ state virtually degenerate with the ground state of **1**.

Several calculations were run on butterfly-type structures **6** with various puckering angles. No minimum could be found, but the potential energy surface seems to be very flat along this deformation coordinate. In this type of bonding interaction, there is a formally double W═Si bond, and delocalized bonding between the heavy atoms and the H's. It turns out that there is a more favorable alternative with a slightly different type of structure. If both H's are bound to W^+ rather than truly bridging (see **6** in Figure 4), it is possible to build a triple bond between W^+ and Si. The five metal valence electrons are therefore involved in covalent bonds, while there remains an unpaired electron on Si. As for **4**, this is a doublet state with C_s symmetry, which required restriction of the CAS space to SDTQ excitations. Optimization of such a structure leads to a WHH plane nearly perpendicular to the W−Si axis. The σ bonds are somewhat delocalized over the entire molecule, while π bonds establish between W^+ and Si along the *x* and *y* directions. This π bonding imposes the condition that the singly occupied orbital be along the *z* axis, leading to a $^2A'$ state. Mulliken populations in the singly occupied MO show that the unpaired electron is mainly localized on Si. The short W−Si bond length of 2.210 Å is consistent with a triple bond, while the W^+−H bond lengths of 1.709 Å are typical, as in previous cases, of single covalent bonds.[14] This isomer lies 23.0 kcal/mol higher in energy than the ground sextet silylene.

In summary, there is a large number of bonding possibilities, leading to several isomers in $WSiH_2^+$. However, there is a single most stable isomer, the high-spin silylene. This is consistent with the CID spectrum, which is indicative of only one structure.

(b) $WSi_2H_4^+$. This ion, which would appear at $m/z = 246$ as the product of single dehydrogenation of the second silane molecule, is not observed. It is difficult to imagine that the two H_2 eliminations leading to $WSi_2H_2^+$ (reaction 4) proceed in a single step. It is much more likely that a first H_2 loss first leads to the formation of $WSi_2H_4^+$. This ion is probably formed with enough internal energy to rapidly lose another H_2 molecule. Calculations were performed on this ion in order to get a better understanding of the course of the second reaction.

Since the results for $WSiH_2^+$ are in favor of structures with hydrogens bound to Si rather than to W^+, three types of geometries can be considered for $WSi_2H_4^+$, as shown in **7**−**9**.

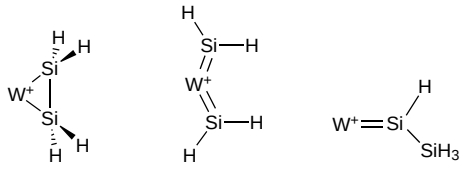

7 **8** **9**

In the quartet states of **7** there are three unpaired electrons on W^+, and as in $WSiH_2^+$, they can be arranged in four orbitals. The d_{xy} and d along the *y* axis lead to the lowest repulsion with the bonding electrons and are each singly occcupied. There remains one high-spin electron to be placed either in the d_σ in the *xz* plane or in the d_{yz} orbital, leading to $^4A_2$ and $^4B_2$ states, respectively. The active space includes the W−Si and the Si−Si bond pairs (with one bonding and one antibonding orbital for the treatment of each) plus the high-spin electrons at W^+ in each case. The $^4B_2$ state was found to lie significantly lower

(48) Examples of distortions in unsaturated silicon compounds: Colegrove, B. T.; Schaefer, H. F. *J. Phys. Chem.* **1990**, *94*, 5593. Grev, R. S.; Schaefer, H. F. *J. Chem. Phys.* **1992**, *97*, 7990. Grev, R. S. *Adv. Organomet. Chem.* **1991**, *33*, 125. Raghavachari, K. *J. Chem. Phys.* **1988**, *88*, 1688. Jemmis, E. D.; Prasad, B. V.; Tsuzuki, S.; Tanabe, K. *J. Phys. Chem.* **1990**, *94*, 5530. Trinquier, G. *J. Am. Chem. Soc.* **1992**, *114*, 6807; *Chem. Phys. Lett.* **1992**, *188*, 572. Treboux, G.; Trinquier, G. *Inorg. Chem.* **1992**, *31*, 4201. Kutzelnigg, W. *Angew. Chem., Int. Ed. Engl.* **1984**, *23*, 272. Koseki, S.; Gordon, M. S.; Schmidt, M. W. *Chem. Phys. Lett.* **1992**, *200*, 303.

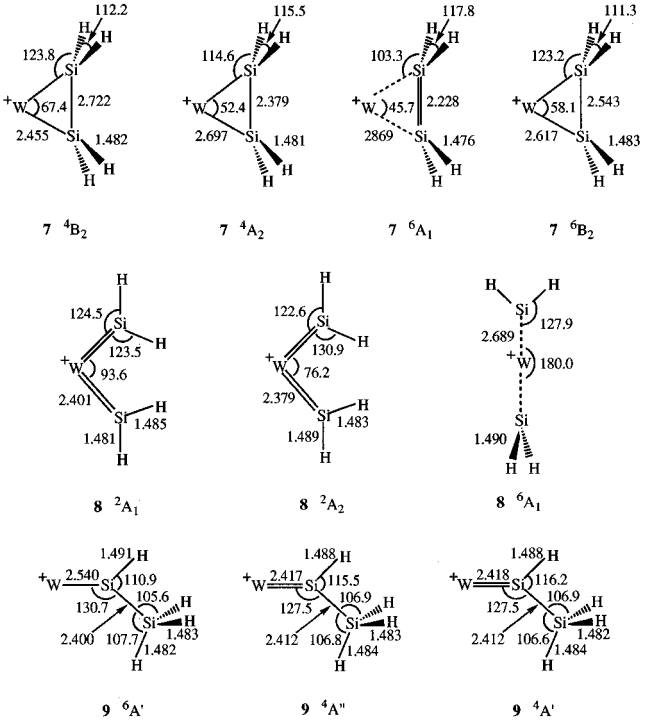

Figure 5. Optimized geometries for various electronic states of $WSi_2H_4^+$ isomers.

Table 3. Energies of Various Electronic States of $WSi_2H_4^+$ Isomers, Optimized at the CASSCF Level (See Text)

isomer and state	CSF[a]	total energy[b]	rel energy[c]
7 $^4B_2$	1456	−76.674 146	0.0
7 $^4A_2$	1520	−76.637 469	23.0
7 $^6A_1$	321	−76.653 401	13.0
7 $^6B_2$	309	−76.633 621	25.4
8 $^2A_1$	2220	−76.630 492	27.4
8 $^2A_2$	2200	−76.598 201	47.7
8 $^6A_1$	1215[d]	−76.637 859	22.8
9 $^6A'$	612	−76.670 114	2.5
9 $^4A''$	2912	−76.646 770	17.2
9 $^4A'$	2848	−76.644 534	18.6

[a] Number of Configuration State Functions included in each case. [b] Total energies in atomic units (hartrees). [c] Relative energies in kcal/mol. [d] In C_1 symmetry.

in energy than the $^4A_2$, and the optimized equilibrium structures of the two states are quite different (see Figure 5 and Table 3).

Recalling that Si−S single and double bond lengths are 2.38 and 2.13 Å in $H_3Si-SiH_3$ and $H_2Si{=}SiH_2$, respectively, it appears that a typical Si−Si single bond exists in the $^4A_2$ state. Actually the WSiSi metallacycle is similar to the experimental structure in $(\eta^5\text{-}C_5H_5)_2WSi_2Me_4$ where W−Si = 2.606 Å and Si−Si = 2.260 Å.[49] It is also close to the structure computed for $Cl_2WSi_2H_4$.[50]

The situation is quite different in the $^4B_2$ ground state with shorter W−Si bonds and a very long Si−Si bond. In fact the W−Si bond length is not much larger than in **1**, the basic silylene structure. The Si−Si bond is so long that this state is better viewed as a face-to-face bis-silylene complex with interacting ligands.

Given the special stability of the sextet silylene complex in $WSiH_2^+$, sextet disilene states were computed for **7**. Here again, the metal has five singly occupied and one empty valence orbitals. However, the situation is less favorable than in $WSiH_2^+$ since two metal orbitals point toward the disilene, a s/d_{z^2} hybrid (directed at the middle of the Si═Si bond) and the d_{xz} (pointing toward both Si atoms), out of which one has to be occupied. If the σ metal orbital is left empty, a $^6A_1$ state is obtained. This allows for efficient charge transfer from the π bond of disilene to the metal, since the metal charge is reduced to +0.33. However, bonding W−Si interactions are prevented by the high-spin electron in the d_{xz} orbital. This leads to long W−Si bonds (2.869 Å) and a short, nearly double, Si−Si bond of 2.228 Å. The second alternative is to leave the d_{xz} metal orbital empty, resulting in a $^6B_2$ state with bonding characteristics opposite to those of the $^6A_1$. There is now an increase in W−Si binding, as shown by the shorter W−Si bonds (2.617 Å) and longer Si−Si (2.543 Å) bonds. However, the high-spin σ electron on W^+ limits the charge transfer interaction, as illustrated by the metal charge of +0.43. The balance of these two effects is in favor of the $^6A_1$ state, which is computed to be 12.4 kcal/mol more stable than the $^6B_2$ state. However, the need for a compromise between the two types of interaction makes the $^6A_1$ state less stable than the $^4B_2$ state by 13.0 kcal/mol. It can be argued that metal cations having the same ability as W^+ to make strong bonds but bearing fewer valence electrons, such as Hf^+ and Ta^+, should make stronger bonds to disilene. This is true for both covalent binding in a low spin state (because the loss of exchange stabilization on the metal would be reduced) and dative bonding in a high-spin state (because there would be no metal electrons "in the way").

The planar bis-silylene structure **8** involves two doubly bonded SiH_2 groups. The W−Si σ bonds use the metal s (in-phase combination) and d_{xz} (out-of-phase combination) orbitals. The π bonds use the d_{yz} (in phase combination) and the d_{xy} (out-of-phase combination) orbitals. Thus there remains one nonbonding electron at W^+ leading to doublet states. It can be placed in any combination of the $d_{x^2-y^2}$ and d_{z^2} orbitals. The lowest repulsion with bonding orbitals is obtained with a d_σ singly occupied in the *xz* plane, corresponding to a $^2A_1$ state. The optimum structure has W−Si bond lengths nearly equal to that in the mono-silylene **1**. It is anticipated that states of any other symmetry will lie higher in energy since they must bear the nonbonding electron in one of the bonding metal orbitals described above. This was verified by computing the $^2A_2$ state, in which the out-of-phase combination of π W−Si bonds is replaced by an in-phase function, in order that the d_{xy} orbital of W^+ be singly occupied. This state is indeed found to lie 20.3 kcal/mol higher in energy than the $^2A_1$ state. There is distorted bonding in this state, since the singly occupied orbital partially delocalizes onto the Si atoms in order to maintain some degree of π bonding; this leads to W−Si bonds slightly shorter than in the $^2A_1$ state, even though the bonding interaction is weaker. The new σ bonding orbital builds in some Si−Si bonding character, which explains why the angle at W is smaller than in the $^2A_1$ state. It can be anticipated that similar destabilizations occur in the lowest $^2B_1$ and $^2B_2$ states.

Since the mono-silylene complex is most stable in the sextet state, the lowest sextet of the bis-silylene was also considered. As in **1**, binding occurs between the metal in a $^6A_1$ state, with two singlet SiH_2 groups able to donate electrons from their σ lone pairs. This interaction is most stabilizing if the lone pairs can point toward the empty metal orbital. The optimum structure is therefore linear, since it also minimizes the repulsion between the SiH_2 groups. The latter can be best relieved when both groups lie in perpendicular planes; however, since the Si−Si distance is very large, the potential energy surface is very flat in this area. The $^6A_1$ state is found to be more stable than the lowest doublet state of **8**, but it still lies 22.8 kcal/mol higher

(49) Berry, D. H.; Chey, J. H.; Zipin, H. S.; Carroll, P. J. *J. Am. Chem. Soc.* **1990**, *112*, 452.
(50) Cundari, T. R.; Gordon, M. S. *J. Mol. Struct. (Theochem)* **1994**, *313*, 47.

in energy than the ground state of **7**. The reason for this sextet state being less favorable compared to that of the mono-silylene complex is the competition between the two σ donation interactions, which leads to higher electron repulsion on the metal center. The metal charge is +0.28, corresponding to a total donation of 0.72 electron from both silylene groups, much less than twice that of a single silylene (0.47 electron). As a result, the W−Si bonds are significantly longer. For the same reason, a mixed state with one silylene doubly bonded to W^+ with the other in its ground singlet state, leading to an overall quartet, is even higher in energy and the results are not reported here.

Finally the silylsilylene structure **9** was considered. For the quartet states, the active space included the W−Si σ and π bond pairs plus the Si−Si single bond pair, with the usual bonding/antibonding orbitals for the description of each pair, plus the metal nonbonding electrons. Their electronic structure at W^+ is very similar to that of the quartet states of **1**, except that symmetry is now reduced to C_s. The lowest quartet state of **9** is a $^4A''$ involving d_{xz}, d_{xy}, and s + d_σ as singly occupied metal orbitals. It is therefore analogous to the $^4B_1$ state of **1**. The W−Si bond lengths are nearly the same, and the Si−Si bond length is typical for a single bond. The excited $^4A'$ is deduced from the $^4A''$ by replacing the singly occupied d_{xy} orbital by the $d_{x^2-y^2}$. It is therefore analogous to the $^4B_2$ state of **1**. As in **1**, both states have nearly identical geometries and energies.

The similarity between the quartet states of **1** and **9** suggests that the ground state of **9** may also be a sextet. This is confirmed by the computations. The best combination of five singly occupied orbitals on W^+ is the same as for **1**, leading to a $^6A'$ state. Its optimum geometry has a W−Si bond length of 2.540 Å, very similar to the 2.552-Å value in **1**. The metal charge is +0.51, again very close to that in **1** (+0.53). The $^6A'$ state is the ground state of **9**, 14.7 kcal/mol more stable than the value for $^4A''$. It is only 2.5 kcal/mol higher in energy than the ground $^4B_2$ state of the metallacycle complex **7**. In the absence of complementary experimental information, it is impossible to decide from the present results which is the ground state of $WSi_2H_4^+$.

(c) $WSi_2H_2^+$ (m/z = 244). $WSiH_2^+$ was isolated in the reaction cell and allowed to react with SiH_4 to form $WSi_2H_2^+$. The decay kinetics yielded a rate constant for reaction 4 of 9×10^{-10} cm^3 molecule^{-1} s^{-1}, indicating that the reaction proceeds at close to the collision rate. The CID spectrum of $WSi_2H_2^+$ shows a dominant loss of H_2, plus a minor loss of Si_2H_2. A number of structures can be envisioned for this ion. Based on the results obtained for $WSiH_2^+$, structures having one or both hydrogens attached to W^+ have not been considered in ab initio calculations of $WSi_2H_2^+$. This is also based on the assumption that the reactive species should bear at least two nonbonding electrons on the metal in order to be able to insert exothermically into the Si−H bond of a further silane molecule.

Since silicon is known to make either two or four bonds in stable compounds, there remain three cyclic structures **10**−**12**,

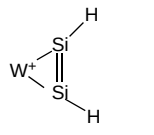

10

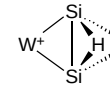

11

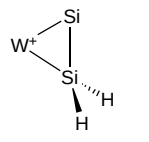

12

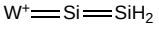

13

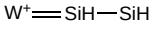

14

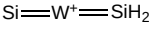

15

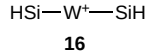

16

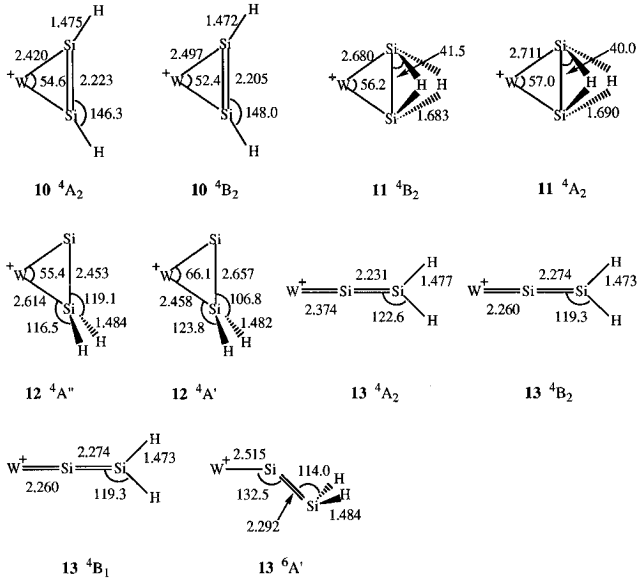

Figure 6. Optimized geometries for various electronic states of $WSi_2H_2^+$ isomers.

two open structures based on the W−Si−Si backbone **13** and **14**, and two open structures based on Si−W−Si, **15** and **16**. It is expected that structures **13**−**16** would lead to loss of either Si, SiH, and/or SiH_2 in the CID spectrum. In the absence of any such loss, we conclude that the most likely are the cyclic structures in which the additional W−Si bond (compared to open structures) probably outweighs any cyclic strain energy.

Calculations were performed on structure **10**, correlating the two W−Si bonds plus the σ and π Si−Si bonds. As before, there are three unpaired electrons on W^+, which lead to two low-lying quartet states. A $^4A_2$ is formed with d_{xy}, s + d_σ along y, and d_σ in the xz plane singly occupied. Replacing $d_{z^2-x^2}$ by d_{yz} leads to a $^4B_2$ state. The ground state was found to be the $^4A_2$ state, lying 15.2 kcal/lmol below the $^4B_2$ state. Their geometries are similar, with Si−Si bond lengths somewhat longer than that of free disilene, probably due to the relaxation of cyclic strain. The $^4A_2$ state is stabilized by mixing of the tungsten d_{yz} orbital with the π Si−Si bond. In the $^4B_2$ state, the d_{yz} orbital is singly occupied and has to be orthogonal to the π bond. As a result, the W−Si bonds are longer by 0.077 Å in the $^4B_2$ state.

Structure **11** is nonclassical, and was investigated since it contains a Si_2H_2 ligand that has a structure of lower energy than the acetylene-like structure for free Si_2H_2.[44] As for **10**, $^4A_2$ and $^4B_2$ states were investigated, with essentially identical nonbonding character at W^+ as those described above. The π Si−Si bond is disrupted in favor of an out-of-phase combination of Si−H bonds. For the other bonds, hybridization of the Si orbitals cannot be optimal for the W−Si, Si−Si, and Si−H bonds simultaneously. For instance, starting with a doubly bridged Si_2H_2 species, there is no Si orbital pointing toward the metal. As a result, there is a decrease of all bonding interactions as compared to the states of isomer **10**, and a lengthening of all bonds is associated as seen in Figure 6. Because of this competition between several bonding alternatives, both states of **11** are significantly higher in energy than those of **10**.

Given the well-known ability of silicon to make stable compounds with only two bonds (keeping a nonbonding pair on Si), low-lying states of **12** were computed. As for previous isomers, the s and d_{xz} metal orbitals are involved in forming W−Si σ bonds. Here symmetry is lowered to C_s, so that states of $^4A'$ and $^4A''$ symmetry emerge. In the latter, the singly

Table 4. Energies of Various Electronic States of $WSi_2H_2^+$ Isomers, Optimized at the CASSCF Level (See Text)

isomer and state	CSF[a]	total energy[b]	rel energy[c]
10 $^4A_2$	20 531	−75.489 612	0.0
10 $^4B_2$	20 435	−75.465 266	15.2
11 $^4A_2$	21 035	−75.437 684	32.6
11 $^4B_2$	20 355	−75.447 288	26.6
12 $^4A''$	27 408	−75.470 544	12.0
12 $^4A'$	27 128	−75.513 869	−15.2
13 $^6A'$	12 112	−75.488 498	0.7
13 $^4A_2$	20 627	−75.486 185	2.2
13 $^4B_2$	20 531	−75.470 236	12.2
13 $^4B_1$	20 451	−75.470 234	12.2

[a] Number of Configuration State Functions included in each case. [b] Total energies in atomic units (hartrees). [c] Relative energies in kcal/mol.

occupied metal orbitals are d_{yz} (with a minor amount of d_{xy} mixed in, which was impossible in **10** and **11** due to C_{2v} symmetry), $s + d_\sigma$ along *y*, and d_σ in the *xz* plane. The optimized structure corresponds to the expected single bonds between heavy atoms, and lies 12 kcal/mol higher than the ground state of **10**. The situation is quite different in the $^4A'$ state, with shorter W−Si and longer Si−Si bonds. Here the d_σ (*xz* plane) singly occupied orbital of the $^4A''$ state is replaced by the d_{xy} orbital, actually leading to a pair of rotated orbitals, $d_{xy} + d_{yz}$ and $-d_{xy} + d_{yz}$, with the latter being significantly delocalized onto the empty p_y orbital of the two-bonded silicon atom. The contrasted electronic structures of these two states are not without analogy with those of the two states of structure **7** of $WSi_2H_4^+$.

The extra electron delocalization that is present in the $^4A'$ state leads to an important gain in stability, large enough to make it the lowest energy isomer of $WSi_2H_2^+$ at the CASSCF level (see Table 4). It should be noted, however, that test CI calculations of the **12** $^4A'$ and **10** $^4A_2$ states lead to nearly equal energies. Thus it is probably safe to consider that the lowest states of **10** and **12** are about equally accessible energetically.

In order to check whether cyclic structures are significantly more stable than open ones, calculations were also carried out for the low-lying states of **13**, which is expected to be the lowest open structure because it has multiple bonds between heavy atoms and high exchange energy on the metal. The expected low-energy quartet states are $^4A_2$, $^4B_1$, and $^4B_2$, of the same type as those for isomer **1** of $WSiH_2^+$. The π system of each state is similar to that in allene, i.e. it is comprised of two adjacent bonds in perpendicular planes. With the two hydrogen atoms lying in the *xz* plane, the Si−Si π bond is along the *y* axis, and therefore the W−Si π bond is along the *x* axis (thus the symmetry labels are different in **13** and **1** which has the W−Si π bond along the *y* axis). There is a significant interaction between some metal orbitals and the Si−Si bond, so that the ordering of states differs in **13** and **1**. In the former the lowest state is the $^4A_2$, with d_{xy}, $s + d_\sigma$ in the *yz*, and d_σ in the *xy* plane singly occupied. The W−Si bond length is close to that in **1**, and the Si−Si is an elongated double bond. The special stability of this state arises from an extensive delocalization of the Si−Si π bond through mixing with the metal d_{yz} orbital. In the other two states, d_{yz} is singly occupied so that delocalization is much weaker and leads to reduced exchange stabilization on W^+.

As in $WSiH_2^+$, the lowest state of the silicon ligand (here $SiSiH_2$) is a singlet,[51] which led us to suspect that the ground state of **13** might also be a high spin sextet. Using the same orbital occupations as in **1** leads to a $^6A_1$ state. The geometry of this state was optimized in C_{2v} symmetry as for the above quartets, but just as for the sextet state of **1**, vibrational frequency calculations showed that the actual minimum has C_s symmetry. The optimized structure (see Figure 6) has a W−Si length close to that of the sextet states of **1** and **9**, ca. 0.015 Å longer than in the quartet states. The structure is bent at the central silicon, and strongly pyramidalized at the terminal Si. As in **1**, this is associated with a low frequency for planarization, due to the same tendency for bending as in unsaturated silicon molecules.[47] This sextet is slightly more stable than the $^4A_2$ state in **13**.

The binding of various isomers of Si_2H_2 to WF_4 has recently been studied by Stegmann and Frenking by ab initio computations.[52] These authors found, in agreement with the present results, that the relative stabilities of the various structures are very different from those of the free Si_2H_2 isomers. The disilaacetylene complex was found to be more stable than the dibridged form. Contrary to $WSi_2H_2^+$, they found that no stable $F_4WSiSiH_2$ isomer exists because it can readily be stabilized by a 1,3-F transfer from W to Si, an option which has no equivalent in $WSi_2H_2^+$. These authors also found that the monobridged structure of Si_2H_2, although being the second most stable isomer, does not lead to any stable complex with WF_4. Clearly, optimum binding is widely different in free and metal-bound Si_2H_2. The optimum geometries of analogous isomers of $F_4WSi_2H_2$ and $WSi_2H_2^+$ are qualitatively the same. This similarity arises from the fact that the metal probably has a significant cationic character in WF_4. It should be emphasized, however, that some of the foremost binding characteristics are different in $F_4WSi_2H_2$ and $WSi_2H_2^+$, due to the closed shell electronic structure of the former vs the high spin character of the latter.

The overall conclusion of the above calculations on $WSi_2H_2^+$ is that at least three isomers, **10**, **12**, and **13**, are close in energy and cannot be disregarded as entities formed by the activation of the second silane molecule.

(d) $WSi_3H_2^+$ (m/z = 272). Isolation of $WSi_2H_2^+$ and subsequent reaction with SiH_4 yields a rate constant for reaction 5 of ca. 9×10^{-10} cm^3 molecule^{-1} s^{-1}, close to the collision rate for reaction 4. The CID spectrum of $WSi_3H_2^+$ shows loss of H_2 as the only product. The absence of any ion corresponding to loss of Si_1 and Si_2 fragments strongly argues in favor of a cyclic or polycyclic structure, as discussed below.

B. Fourth to Last Reactions. The fourth reaction constitutes a turning point since it has two distinct products as shown below:

$$WSi_3H_2^+ + SiH_4 \rightarrow WSi_4H_4^+ + H_2 \qquad (6a)$$

$$\rightarrow WSi_4H_2^+ + 2H_2 \qquad (6b)$$

CID experiments were also prevented by the presence of two different ions, $WSi_4H_4^+$ and $WSi_4H_2^+$ with a mass difference of only two units around m/z 300. Selecting either of these ions would lead to significant excitation of the other. This is also the case for all ions with more than four silicon atoms.

From the fifth to the tenth reaction, there appears to be two parallel channels, both involving full dehydrogenation at each step, except for the last which apparently involves a single H_2 loss. This general sequence, leading to $WSi_{10}H_6^+$ and $WSi_{10}H_4^+$ as the ultimate reaction products, is summarized in Scheme 1. This scheme presumes that the last step for each of $WSi_9H_2^+$ and $WSi_9H_4^+$ involves a single dehydrogenation. Alternatively, $WSi_{10}H_4^+$ might also arise from a double dehydrogenation initiated by $WSi_9H_4^+$. However, the similar intensity ratios in

(51) Grev, R. S.; Schaefer, H. F. *J. Chem. Phys.* **1992**, *97*, 7990.

(52) Stegmann, R.; Frenking, G. *Organometallics* **1995**, *14*, 5308.

Scheme 1

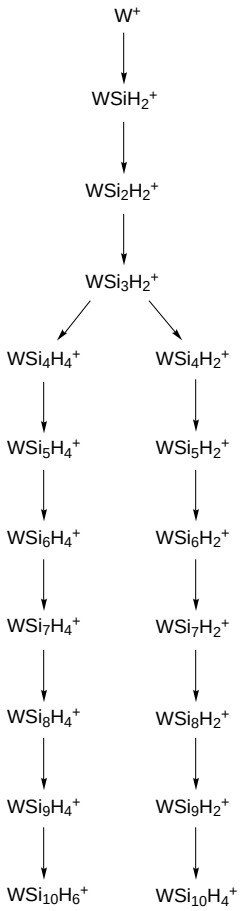

the $WSi_9H_4^+/WSi_9H_2^+$ and $WSi_{10}H_6^+/WSi_{10}H_4^+$ product pairs would indicate that the proposed mechanism is dominant.

At reaction times in the 6−20-s range, relative intensities of $WSi_nH_4^+$ and $WSi_nH_2^+$ are variable depending on *n*; however at longer times $WSi_nH_4^+$ become dominant. The spectrum recorded at the longest time (40 s) is shown in Figure 7. It can be seen that $WSi_{10}H_6^+$ ($m/z = 472$) is the dominant ion, with minor amounts of $WSi_9H_4^+$ ($m/z = 442$) and $WSi_{10}H_4^+$ ($m/z = 470$). There are also a few peaks corresponding to oxygen-containing species, $WSi_6OH_2^+$ ($m/z = 372$), $WSi_7OH_2^+$ ($m/z = 400$), and $WSi_7OH_4^+$ ($m/z = 402$). It should be noted that a small peak corresponding to $WSi_{11}H_6^+$ was observed when experiments were carried out without collisional cooling with argon. With argon, no Si_{11} species was observed. The possibility also exists that an eleventh reaction proceeds with a rate constant several orders of magnitude smaller than for the previous steps.

A high resolution spectrum of the final reaction product is shown in Figure 8. The high-resolution mass assignment and intensity ratios are consistent with that expected from a statistical distribution of silicon in $WSi_{10}H_6^+$. However, given the high pressure of argon used (10^{-6} Torr) and the very long reaction time (40 s), the alternative possibility of a species $WSi_9H_2O_2^+$ cannot be completely eliminated. Nevertheless, since no other species containing two oxygens have been observed, this latter possibility seems unlikely. Therefore, the reaction sequence can fairly confidently be considered to terminate at $WSi_{10}H_6^+$.

Discussion

From the energetic information obtained from the *ab initio* calculations and the structural information which can be inferred from the CID experiments, it is possible to construct a probable mechanism for the extensive series of reactions initiated by W^+.

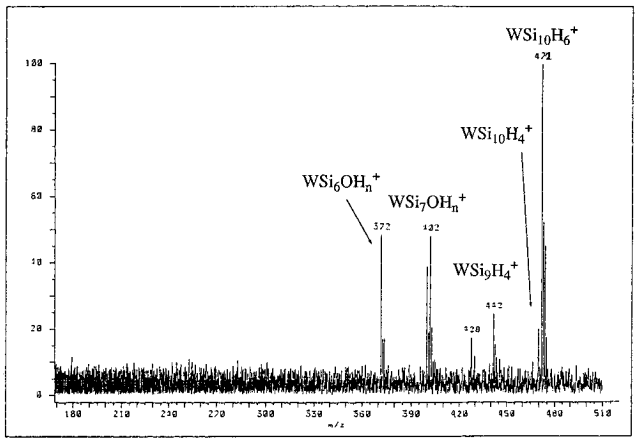

Figure 7. Spectrum after 40 s of reaction in the presence of 10^{-6} mbar of argon.

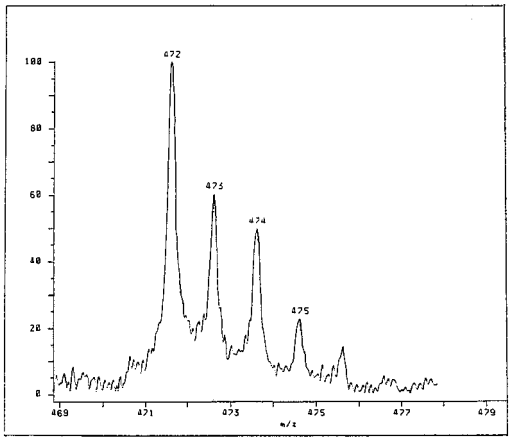

Figure 8. High-resolution spectrum of $WSi_{10}H_6^+$ in the presence of 10^{-6} mbar of argon.

Following the formation of an initial electrostatic complex between W^+ and SiH_4, given the high efficiency of the first reaction, there can be no significant barrier in proceeding to an insertion complex, $HWSiH_3^+$. At this point, following the classical mechanism previously supposed for H_2 elimination, the reaction may follow either a mechanism involving H migration from Si to W^+ followed by reductive elimination or a concerted four-center mechanism (Scheme 2).[17] Ab initio calculations show that the $WSiH_2^+$ product ion has a metal−silylene structure with a sextet spin state.

The $WSiH_2^+$ ion, as described above, reacts further with a second molecule of silane via a mechanism which also presumably begins with insertion in a Si−H bond. This is followed by elimination of H_2 leading to a $WSi_2H_4^+$ species which is not experimentally observed in the course of the reaction. The *ab initio* calculations reveal the possibility of two structures of relatively low energy for $WSi_2H_4^+$, **7** and **9**. The second loss of H_2 gives rise to the observed $WSi_2H_2^+$ ion which has three low-energy structures suggested by the *ab initio* calculations, **10**, **12**, and **13**. The open structure **13**, while still a possibility, might be regarded as being less probable on the basis of failure to observe loss of SiH_2 upon collisional activation (the Si═Si bond being probably weaker than the W═Si bond). There are no strong arguments to eliminate any of the structures **10**, **12**, or **13** since all are consistent with the dominant loss of H_2 in the CID spectra and are compatible with reactivity at the metal

Scheme 2

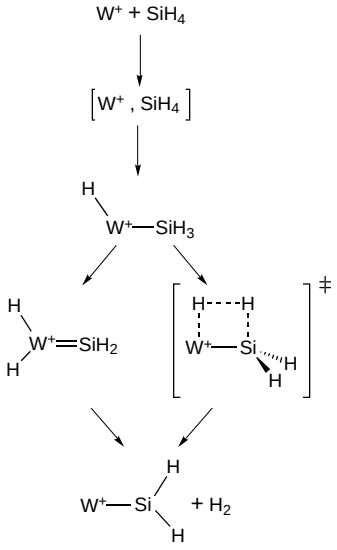

Scheme 3

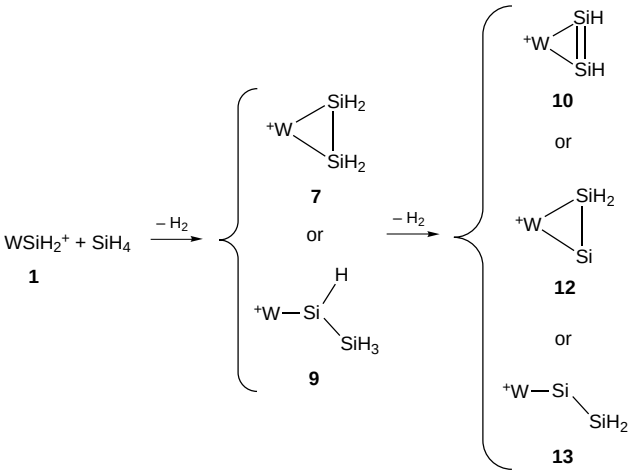

center in the subsequent reaction with SiH_4. The possibilities for the second reaction sequence are outlined in Scheme 3.

The fact that the double dehydrogenation of SiH_4 occurs in the second reaction implies the thermochemical condition that the strength of the new bonds formed (taking account of those in $WSiH_2^+$ and the ring strain) is greater than 100 kcal mol^{-1}, the energy required for the double dehydrogenation. This double dehydrogenation is not observed in the analogous reactions with methane,[9b,13] an effect which is due to the much larger energetic requirement, 189 kcal mol^{-1}.

It should be noted that a very small peak due to WSi_2^+ is also present in the spectrum. This result indicates that a third dehydrogenation is very probably thermoneutral or marginally endothermic. Alternatively, this reaction may be due to a small fraction of $WSiH_2^+$ ions which still contain some fraction of the exothermicity of the first reaction as internal excitation.

The third reaction leads to a further double dehydrogenation. The number of possible structures for $WSi_3H_2^+$ becomes very large, but if only those that are cyclic are considered, eleven structures can be envisaged. This cyclic character of the product would appear to be a logical assumption since the CID spectra of $WSi_3H_2^+$ show only the facile loss of H_2. These eleven possible structures, **17**−**27**, differ only by the position of the

Chart 1

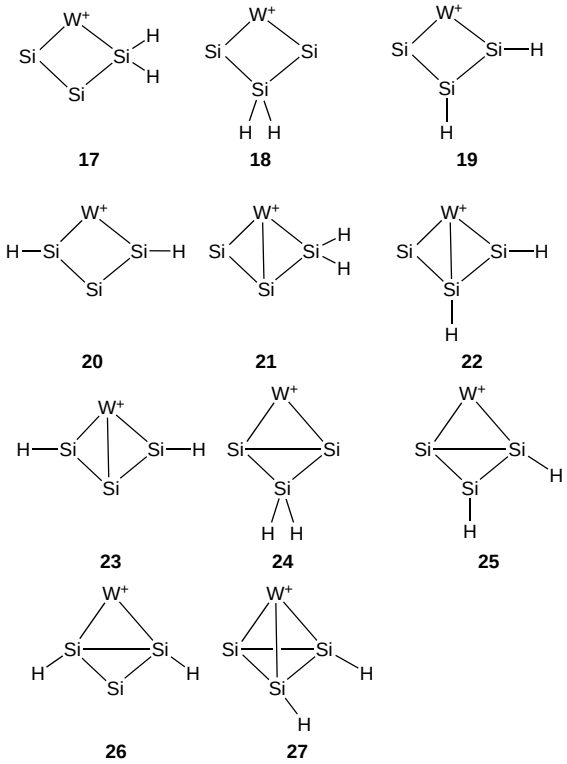

hydrogens and the degree of connectivity between the heavy atoms. It is possible to suggest that the ease with which H_2 is lost upon collisional activation is due to the fact that it is accompanied by a further increase in connectivity between heavy atoms, leading to a very compact structure. Although it is not possible to unambiguously suggest a single structure for WSi_3^+, **28** appears particularly attractive.

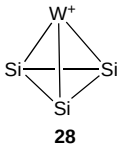

As noted above, the fourth reaction represents a turning point in that $WSi_3H_2^+$ leads to both a single and a double dehydrogenation. One possibility that immediately suggests itself is that there are in fact two or more different $WSi_3H_2^+$ species which react either by single or double dehydrogenation, dependent upon the degree of connectivity. Given the large number of possible $WSi_3H_2^+$ structures proposed above, this is not at all unreasonable. However, two other possible reasons for the appearance of two $WSi_4H_n^+$ products can be suggested. One is that H_2 loss from $WSi_4H_4^+$ is nearly thermoneutral and has no significant barrier. Since one can assume that $WSi_4H_4^+$ ions are formed with some distribution of internal energies, part of them may then be able to undergo further dehydrogenation. Another possibility is that two isomeric $WSi_4H_4^+$ structures are formed, from a single $WSi_3H_2^+$ precursor, with only one undergoing loss of H_2.

In all cases, species with the same formula can differ in electronic state, molecular structure, internal energy, etc. Resolving this alternative could be achieved by monitoring the decay of $WSi_3H_2^+$. This decay would be expected to be well fitted by a single exponential in the first case, and by a superposition of two in the second. Unfortunately, this study turned out to be impossible due to the high reactivity of

$WSi_3H_2^+$ with traces of an oxygen-containing species present in the cell, presumably water.

As noted above, the fifth to the ninth reactions are compatible with the existence of two parallel reaction channels initiated by $WSi_4H_2^+$ and $WSi_4H_4^+$, each proceeding via double dehydrogenation. However, it is also possible that some crossover between these two pathways occurs where the least saturated ion is capable of effecting both a single and a double dehydrogenation in the manner observed with $WSi_3H_2^+$. Given the number and complexity of structures plausible for the $WSi_4H_n^+$ to $WSi_9H_n^+$ products, it is not possible to reasonably suggest either structures for these species or mechanisms for their formation.

Assuming that there are indeed two parallel reaction channels, each of the last reactions proceeds via a single dehydrogenation. The fact that this step is accompanied by a change in the degree of dehydrogenation and leads to the end of the reaction sequence would indicate that the $WSi_{10}H_n^+$ species formed are especially stable, either thermodynamically or kinetically. Two possibilities for this stability can be envisaged. Either, for the first time, the metal no longer has sufficient electrons to insert in a Si−H bond or it has become sterically inaccessible. Although by no means the only possibilities, structures **29** and **30**, based on two Si_{10} structures previously obtained by Raghavachari,[53] satisfy the conditions outlined above.

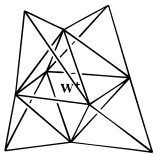

29

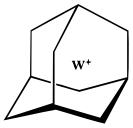

30

The first, a tetracapped octahedron, is based on the Si_{10} structure determined to be of lowest energy. The second is based on an adamantane structure, which, although of considerably higher energy among Si_{10} isomers, presents a sizable cavity capable of accommodating W^+ within. This isomer also has dangling bonds (thus making it less stable), which should enable bonding interactions with the metal, although the pyramidalization at Si centers makes each of them far from optimum.

JA952221O

(53) Raghavachari, K.; McMichael Rohlfing, C. *J. Chem. Phys.* **1988**, *89*, 2219. See also: Messmer, R. P.; Patterson, C. H. *Chem. Phys. Lett.* **1992**, *192*, 277. Raghavachari, K.; McMichael Rohlfing, C. *Chem. Phys. Lett.* **1992**, *198*, 521.